IJME

Int. J. of Applied Mechanics and Engineering, 2025, vol.30, No.2, pp.124-139
DOI: 10.59441/ijame/200965

MHD HYPERBOLIC TANGENT CASSON-WILLIAMSON NANOFLUID OVER A LINEARLY STRETCHING SHEET WITH THERMOPHORESIS AND BROWNIAN MOTION

B. Shashidar Reddy[1], B. Narsimha Reddy[2], K. Saritha[3] and Ch. Chesneau[4*]

[1]Department of Mathematics, Sreenidhi Institute of Science and Technology, INDIA
[2]Department of Science and Humanities, Anurag University, INDIA
[3]Department of Humanities and Science, CVR College of Engineering, INDIA
[4]Mathematics, Université de Caen-Normandie, FRANCE
E-mail: christophe.chesneau@gmail.com

The main aim of this research is to investigate the effects of Brownian motion and thermophoresis on an MHD hyperbolic tangent Williamson-Casson nanofluid passing over a stretching sheet. Through appropriate similarity transformations, non-linear partial differential equations governing the model can give rise to non-linear ordinary differential equations. These equations are solved numerically using the Keller-Box method. The quantities related to engineering aspects, such as skin friction, Sherwood number, heat exchange and the various effects of quantifiers on momentum, temperature, and concentration are illustrated with examples for better understanding. For the sake of accuracy, the computational resolution of this research is limited to the published data and is derived from the Keller-Box approach. Heat exchangers, chemical reactors, and thermal management systems are just some of the technological applications for which the study's conclusions may have broad implications. Skin friction increases with Casson and Williamson parameters. For both the fluids, mass transfer is accelerated with Brownian effect while heat transfer decelerates with thermophoresis effect. The combination of Casson-Williamson characteristics, hyperbolic tangent fluid dynamics and MHD provides a novel way of understanding non-Newtonian fluids in the presence of magnetic fields.

Key words: Casson fluid, Williamson fluid, Brownian motion, thermophoresis, suction, Keller-Box method, Hartmann number, Prandtl number.

1. Introduction

There are many areas of research and development that involve the study of the stretched flow of electrically conducting materials, including plasma research, nuclear power plants, petroleum exploration, and the extraction of heat-trapping energy sources. In addition, there are many technical processes that can be used, such as melting, extrusion, manufacturing of glass fibers, heated rolling wire, the creation of rubber and plastic sheets, and cooling of the vast metallic plate inside an environment that could be an electrolyte, which involves the movement of a stretch surface. When producing the filaments and polymer sheets, they are often extruded by a windup roller that is situated in a die a certain distance away. The flow that flows through a stretching was investigated by Crane [1]. Cortell [2] analyzed non-Newtonian fluid flow on stretching surfaces and employed the shooting technique to come up with a numerical solution to the equation that governs it. Ahmed *et al.* [3] investigated the convective movement in MHD Jeffrey fluid on an extended surface. Imran Anwar *et al.* [4] solved the chemical reaction that occurs on the MHD nanofluid and heat flow across the stretched sheet. Heat conductivity, viscosity, and heat transfer processes in nanofluids were reviewed by Noorzadeh *et al.* [5]. The study of magnetic fields and non-Newtonian fluids has attracted much attention because of their massive applications in science and technology, such as blood flow measurement methods, turbomachinery and nuclear accelerators, as well as heat exchanger design and many related fields. MHD influences on non-Newtonian

* To whom correspondence should be addressed

liquids passing through a plate that is moving were studied by Naikoti and Shashidar [6]. Saritha *et al.* [7] tried to inspect the effects of different variables in the non-Newtonian MHD flows via a porous medium that is dynamically changing. Asogwa and Ibe [8] gave an analysis of the MHD Casson fluid flow across a permeable stretched surface with mass and heat transfer.

Recent research has focused on the study of nanomaterials. This is because of their widespread use in electronics and manufacturing, as well as in medicine and transport. A modern type of fluid, known as a nanofluid, is a fusion of a fundamental fluid with particles of nanotechnology. These nanoparticles consist of a variety of metals, such as copper, silicon, and aluminum. Since the majority of fluids for heat transfer, like oil, water, ethylene glycol, or motor oil, have naturally low conductivity, conventionally, base fluids can have their thermal conductivity enhanced by adding nanoparticles Khan and Pop [9] examined the movement of a nanofluid's boundary layer through the stretched sheet. Kuznetsov and Nield [10] inspected the convection flow of a nanofluid over an elongated vertical plate. Mabood *et al.* [11] developed an algorithmic model of the MHD boundary layer and heat transfer in nanofluids on a non-linear stretching sheet.

The importance of thermal radiation effects and MHD flow issues in basic manufacturing has also increased. Electricity generation, solar power, astrophysical flow technologies, spacecraft re-entry and a variety of other industrial applications all have a similar flow. As the thermal radiation parameter increases and the temperature of the fluid rises rapidly, there will be more fluid in the boundary layer due to buoyancy effects. So this is a way of making the fluid move faster. Akolade *et al.* [12] illustrate how thermophysical characteristics, including chemical and radiative impacts, affect the MHD flow of Casson fluid. Sheikholeslami *et al.* [13] investigated the impact of heat and radiation on MHD free convection of Al_2O_3-H_2O nanofluid. SitiKhuzaimah *et al.* [14] studied the movement of a boundary layer of hydromagnetic energy across a stretched area exposed to heat radiation.

Williamson fluids are non-Newtonian liquids that exhibit thinning of shear (i.e., the viscosity decreases as the rate of strain increases). Hayat *et al.* [15] analyzed the 2D MHD flowing of a Williamson nanofluid on a thickened, nonlinearly fluctuating surface that has melting transfer. Khan *et al.* [16] explored the MHD flow of a Williamson nanofluid on cones and plates with chemicals that react. Malik *et al.* [17] examined the MHD of a hyperbolic, tangentially oriented fluid moving via a stretched cylinder by the Keller-Box technique. Akbar *et al.* [18] showed how a hyperbolic stream flows from a magnetic-hydrodynamic boundary to a stretched sheet by using numerical solutions. With fluctuating viscosity and heat conductivity effects, Idowu *et al.* [19] looked over the MHD heat and mass transfer flow of Casson fluid. Gbadeyan *et al.* [20] investigated the effects of altered heat transfer efficiency and viscosity on the Casson nanofluid flow coupled with convective heat and velocity slip. Many investigators [21-24] presented the effects of several factors on Casson nanofluid flows.

Chemical reactions can have various applications in the industry. Chemical reactions can be used to reuse products, produce lubricant, and create different compounds that could be beneficial to industry. Mabood *et al.* [25] studied the stretched-sheet MHD stagnation flow as well as heat transfer using chemical reactions and transpiration. Hayat *et al.*[26] discussed the convection-mixed flow of chemically reactive Casson nanofluid that is convectively heated, in addition to heat production and absorption on a stretched sheet. Moving across a stretched sheet, the boundary layer flow of an MHD tangent hyperbolic nanofluid was numerically solved by Khan *et al.* [27]. Reddy C *et al.* [28] examined the transport of heat and flow characteristics of the Williamson nanofluid over an adjustable stretching sheet thickness and thermal conductivity. Nadeem and Hussain [29] analyzed the Williamson fluid's heat transmission over an exponentially stretched surface. Li *et al.* [30] Muzara and Shateyi [31], Zhu *et al.* [32] illustrated the heat transfer of Williamson fluid flows.

Two different non-Newtonian fluid systems are used to describe the rheological nature of certain fluids: Casson and Williamson fluids. The fluid flow properties are highly dependent on the governing fluid parameters used in these models. Chemical reactions and heat radiation's effect on the MHD of a Casson and Williamson nanofluid flowing across a porous stretched sheet are investigated by Humane *et al.* [33].

Numerous fields rely on tangent hyperbolic nanofluids for effective heat transfer, including energy and power generation, electronics and microelectronics, biomedical engineering, industrial systems, and many more. The impact of different parameters on tangent hyperbolic nanofluid flows was investigated by several researchers [34-39]. Pattnaik [40] studied the radiative and dissipative heat effect on the Williamson nanofluid flow due to thermal buoyancy. Influence of various parameters on nanofluid were discussed by the several authors [41-43]. Yousef *et al.* [44] studied Casson-Williamson nanofluid movement across a slick extended sheet through a porous material. Free convection of conducting nanofluid with heat source was investigated by Baag [45]. Several studies [46-48] illustrated the studies related to Hybrid nanofluid. Anwar *et al.* [49] demonstrated the two-dimensional fluid flow that contains nanoparticles with MHD hyperbolic tangents to the stretching sheet.

Enhanced thermal management, fluid flow efficiency, and accuracy in small-scale systems are just a few of the many practical applications that benefit greatly from a solid grasp of the tangent hyperbolic nanofluid flow geometry and its implications for heat transfer behavior. The current work, which aims to understand the boundary layer flow of hyperbolic tangent Williamson-Casson nanofluid across a stretched sheet, is motivated by the previously described research. Further details and motivations are given in the next section.

2. Model formulation

Let us consider a tangent hyperbolic nanofluid that flows continuously and is incompressible inside a 2D- boundary on a sheet that is stretched linearly with a surface that is the $y = 0$ point and the velocity in the range of $u_W = ax$. The fluid flow is in a vertical direction in relation to the magnetic fields with a force of $B_0{}^2$ and occurs within the region where $y > 0$. Since it is likely that the Reynolds number is small, the magnetic field also appears to be small. On the extending surface, we assume that the wall temperatures T_w as well as the nanoparticle percentage of C_W are both constant. The temperature as well as the proportion of nanoparticles in the air are represented by the letters T and C, as the y value is infinity.
To have a graphical benchmark, Fig.1 presents the physical model and coordinate system.

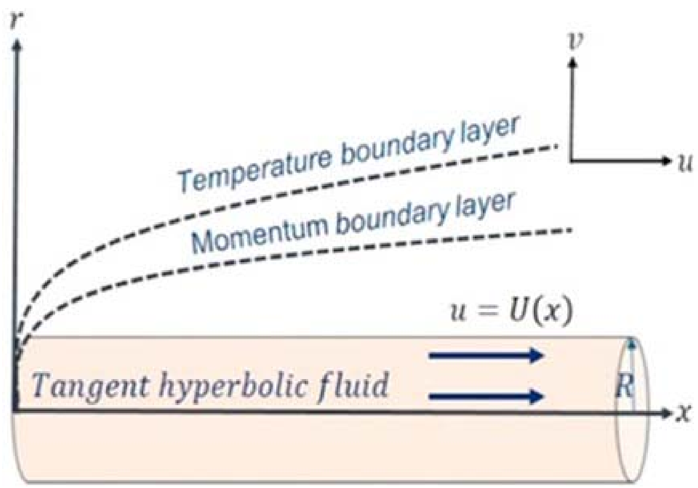

Fig.1. Physical model and coordinate system [50].

The mathematical model based on boundary layer assumptions (Haq *et al.* [23]) is provided below.

$$\frac{\partial u}{\partial x}+\frac{\partial v}{\partial y}=0\,, \tag{2.1}$$

$$u\frac{\partial u}{\partial x}+v\frac{\partial u}{\partial y}=v\left(1-n+\frac{1}{\beta}\right)\frac{\partial^2 u}{\partial y^2}+\sqrt{2}\Gamma\nu n\frac{\partial u}{\partial y}\frac{\partial^2 u}{\partial y^2}-\frac{\sigma B_0{}^2 u}{\rho}\,, \tag{2.2}$$

$$u\frac{\partial T}{\partial x}+v\frac{\partial T}{\partial y}=\alpha\frac{\partial^2 T}{\partial y^2}+\tau\left\{D_B\frac{\partial C}{\partial y}\frac{\partial T}{\partial y}+\frac{D_T}{T_\infty}\left(\frac{\partial T}{\partial y}\right)^2\right\}, \tag{2.3}$$

$$u\frac{\partial c}{\partial x}+v\frac{\partial c}{\partial y}=D_B\frac{\partial^2 C}{\partial y^2}+\frac{D_T}{T_\infty}\frac{\partial^2 T}{\partial y^2}. \tag{2.4}$$

The required boundaries are given by

$$\begin{aligned}&y\to 0: u_w=axandv=v_w, \quad T=T_w, \quad C=C_w,\\ &y\to\infty: u=0, \quad T=T_\infty, \quad C=C_\infty.\end{aligned} \tag{2.5}$$

The boundary conditions at $y=0$ show a wall with a constant concentration, a constant temperature, and varying velocity in x-direction. These conditions indicate a forced or shear-driven convection process with wall-fixed mass and thermal characteristics. As y approaches infinity, the vertical velocity stops being a function of y, and the temperature and concentration are close to constant values, suggesting that the free-stream fluid is homogeneous and unaffected by the wall at long distances.
In order to reduce the model equations to a dimensionless form, these transformations are defined on the basis of the methodology of (Akbar *et al.* [18]):

$$\begin{aligned}&\eta=y\sqrt{\frac{a}{v}}, \quad \Psi=\sqrt{a\nu}xf(\eta), \quad u=axf'(\eta),\\ &\theta(\eta)=\frac{T-T_\infty}{T_w-T_\infty}, \quad \phi(\eta)=\frac{C-C_\infty}{C_w-C_\infty}\end{aligned} \tag{2.6}$$

where $u=\dfrac{\partial\Psi}{\partial y}, \quad v=-\dfrac{\partial\Psi}{\partial x}$.
Substituting Eq.(2.6) into Eqs (2.1)-(2.4), we obtain:

$$\left(1-n+\frac{1}{\beta})+nWef''\right)f'''-f'^2+ff''-M^2f'=0, \tag{2.7}$$

$$\theta''+Pr(f\theta'+Nb\phi'\theta'+Nt\theta'^2=0, \tag{2.8}$$

$$\phi''+PrLef\phi'+\frac{Nt}{Nb}\theta''=0. \tag{2.9}$$

The modified boundaries are

$$\left.\begin{aligned}&f(0)=S, \quad f'(0)=1, \quad \theta(0)=1, \quad \phi(0)=1,\\ &f'(\infty)\to 0, \quad \theta(\infty)\to 0, \quad \phi(\infty)\to 0\end{aligned}\right\} \tag{2.10}$$

where the prime denotes differentiation with respect η.

$$M=\frac{\sigma B_0^2}{a\rho}, \quad Pr=\frac{v}{\alpha}, \quad Nb=\frac{(\rho c)_p D_B (C_w-C_\infty)}{(\rho c)_f v}, \quad Le=\frac{\alpha}{D_B},$$

$$Nt=\frac{(\rho c)_p D_T (T_w-T_\infty)}{(\rho c)_f T_\infty v}, \quad We=\Gamma x\sqrt{\frac{2a}{\nu^3}}. \tag{2.11}$$

The Sherwood number, Nusselt number, and local skin friction, which are of particular relevance and significance, are indicated as:

$$Sh_x=\frac{xq_m}{D_B(C_w-C_\infty)}, \quad Nu_x=\frac{xq_w}{k(T_w-T_\infty)}, \quad C_{fx}=\frac{\tau_w}{\frac{1}{2}\rho u_w^2} \tag{2.12}$$

where $$\tau_w=\mu\left(1-n+\frac{1}{\beta}\right)\left[\frac{\partial u}{\partial y}\right]_{y=y_0}+\mu\frac{n\Gamma}{\sqrt{2}}\left[\frac{\partial u}{\partial y}\right]_{y=y_0}^3,$$

$$q_w=-k\left[\frac{\partial T}{\partial y}\right]_{y=y_0}, \quad q_m=-D_B\left[\frac{\partial C}{\partial y}\right]_{y=y_0}. \tag{2.13}$$

With the use of scaling variables, these quantities are modified as:

$$\frac{Re_x^{1/2}C_{fx}}{2}=\left(1-n+\frac{1}{\beta}\right)f''(0)-\frac{nWe}{2}f''^3(0),$$

$$Re_x^{1/2}Nu_x=-\theta'(0), \quad Re_x^{1/2}Sh_x=-\phi'(0) \tag{2.14}$$

where $Re_x=xu_w/v$ is Reynold number.

Following the methods outlined by (Anwar *et al.* [49]), Keller-Box method–which includes the finite differences method, Newton's scheme, and the block elimination process–makes sense of the converted non-linear ordinary differential equations in Eqs (2.7), (2.8), and (2.9), and boundary conditions in Eq.(2.10). This approach has been widely used and seems to be more adaptable than other methods. It is said to be more efficient, less time consuming, easier to program and easier to practice.

3. Solution methodology

Due to the non-linearity of Eqs (2.7), (2.8), and (2.9), it can be difficult to discover a closed-form answer. Using the Keller-Box approach, which involves finite differences, equations are solved numerically with boundaries in Eq.(2.10). The Keller-Box method [51] generally involves the following steps to obtain numerical answers:

Step 1

Applying the substitutions $f'=p,\ p'=q,\ \theta'=t,\ \phi'=g$.

All of the ODEs must be transformed into 1st order ODEs in the early stages.

Step 2: *Separation of domain*

The rectangle grid in $x-\eta$ plane is deliberated in Figure III, and the grid points are demarcated as:

$x^0 = 0, x^i = x^{i-1} + k_i, i = 1,2,3,\ldots\ldots I$,

$\eta_0 = 0, \eta_j = \eta_{j-1} + h_i, j = 1,2,3,\ldots\ldots J$

where (k_i, η_j) are the $\Delta x and \Delta\eta$ step length.

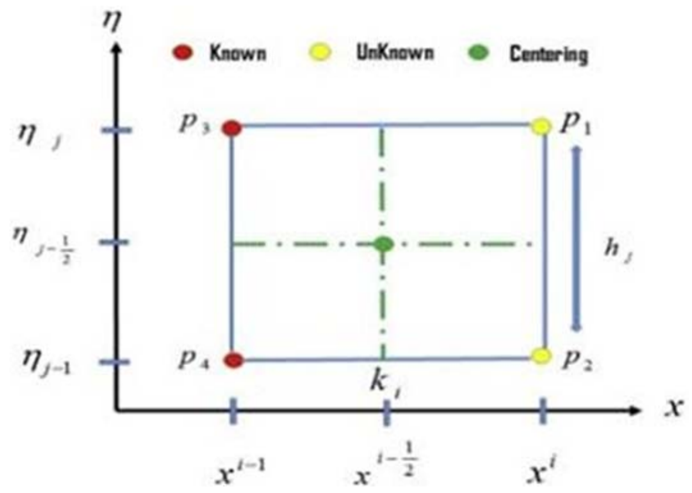

Fig.2. Grid point labelling.

Step 3: *Newton's technique of linearization*

As a consequence of Newton's method, the $(i + 1)^{th}$ iterations of the formulae may be found in the preceding equations

$$(\,)_j^{(i+1)} = (\,)_j^{(i)} + \delta(\,)_j^{(i)}$$

and after overlooking the higher-elevated bounds of $\delta(\,)_j^{(i)}$ a linear tri-diagonal equation scheme.

Step 4: *The bulk scheme and eliminating*

The equation $F\delta = r$ has finally resulted in a bulk tri-diagonal matrix.

Where

$$F = \begin{bmatrix} A1C1 \\ B2\,A2\,C2 \\ \ddots\ddots\ddots \\ \ddots\ddots\ddots \\ B_{j-1}A_{j-1}C_{j-1} \\ B_j A_j \end{bmatrix}, \quad \delta = \begin{bmatrix} \delta_1 \\ \delta_2 \\ \vdots \\ \\ \vdots \\ \delta_{j-1} \\ \delta_j \end{bmatrix}, \quad r = \begin{bmatrix} (r_1)_{j-\frac{1}{2}} \\ (r_2)_{j-\frac{1}{2}} \\ \vdots \\ \\ \vdots \\ (r_{j-1})_{j-\frac{1}{2}} \\ (r_j)_{j-\frac{1}{2}} \end{bmatrix}$$

where F is 7×7 block-sized matrix that corresponds to the size $J \times J$. However, $\delta and r$ are the vector a of order $J \times 1$. Now an efficient LU factorizing process is applied to solve for δ. In $F\delta = r$, F is splinted into lower and upper trigonal matrices, i.e. $F = LU$.

The majority of the numbers required are accurate to within 4 decimal places, according to the tables. This is made possible through a consistent grid with the width of $\Delta\eta = 0.006$ and a precision of 10^{-5}.

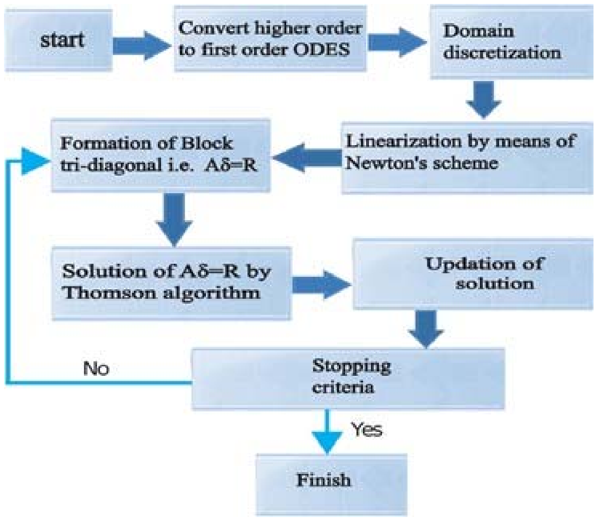

4. Findings and interpretation

Sherwood number, Nusselt number, and skin friction quantities for a variety of different quantitative terms are provided to give a physical insight into this problem. Table 1 represents the deviation of the skin friction coefficient with the Hartmann number. Measuring the skin friction force relative to the fluid's dynamic pressure yields the skin friction coefficient C_f. Note that the skin friction coefficient is directly proportional to the Hartmann number. To examine how skin friction changes in response to changes in n, We, β, and M, we may look at Tab.2. As the power law index n improves, the skin friction decreases, but as the Hartmann number increases, the skin friction improves. The skin friction coefficient accelerates at lower values of the Casson nanofluid parameter β, while the opposite relationship is observed for the Williamson parameter We.

The effect of various physical variables on mass and heat transfer rates is shown in Tab.3. In contrast to Pr, which shows an increasing relationship, the heat transfer rate decreases as Le, β, Nt, Nb, and S are increased. The controlling quantitative terms Le, β, Nt, Nb, S, and Pr all have an increasing effect on the mass transfer rate.

A graphical representation of the effect of controlling fluid properties on Casson and Williamson fluids is presented for a clear understanding of the problem. As can be seen in Fig.2, the Hartmann number has an effect on the velocity profiles for both Casson and Williamson fluids. The Hartmann number of a fluid is a measure of the ratio of its Lorentz force to its viscous force. A high Hartmann number indicates that the fluid is slowed down by the magnetic field, which dominates its motion. The consequence is that the velocity of the fluid decreases as M increases, as shown in Fig.2. Unlike the Williamson fluid, the Casson fluid is clearly found away from the boundary. Figure 3 shows how the power law index affects the velocity. One way of quantifying the shear behavior of the fluid is to look at its power law index, n. As can be seen in the figure, the velocity decreases as n increases. Therefore, the fluid undergoes a transition from shear thinning to shear thickening as n increases. It can be seen from the graph that the power law index has a more significant effect on the Casson fluid than on the Williamson fluid.

The effect of the Weissenberg number We on the velocity profiles can be seen in Fig.4. The graph clearly shows that the velocity profile decreases as the Weissenberg number increases. This is because higher values of the Weissenberg number increase the relaxation time of the fluid particles, which in turn increases the viscosity, which in turn decreases the fluid velocity because it creates more resistance to the flow of the fluid. Compared to Casson's fluid, this effect is quite minimal in Williamson's fluid. As the thermophoresis variable increases, the temperature of the fluid increases, as shown in Fig.5. In fact, the fluid will move from the heated region to the cooled region if the thermophoresis quantifier is high enough to exert a strong enough thermophoretic force on the particles.

The effect of changing the Brownian motion parameter on the temperature is shown in Fig.6 and it is clear from the plot that the temperature of the fluid increases as *Nb* increases. This is due to the fact that when the Brownian motion component is large, there is an increase in the ambient temperature of the fluid, as the component is subject to a large amount of Brownian motion and may move irregularly independent of the fluid flow. The effect of changing the thermophoresis parameter on the final fluid concentration is shown in Fig.7. Increasing the parameter causes the fluid concentration to increase, as can be seen from the graph. The potential effect of Brownian motion on fluid concentration is shown in Fig.8. The concentration decreases as *Nb* increases, as can be seen in the figure.

The influence of the suction/injection variable (*S*) on velocity, temperature and concentration is plotted independently in Figs 9, 10 and 11. It can be seen from these plots that the velocity, temperature and concentration fields all decrease as the suction/injection parameter increases. A suction mechanism is used to suck a certain volume of fluid particles into the wall. As the suction/injection parameter increases, the thicknesses of the momentum, temperature and concentration boundary layers all decrease.

The role of skin friction in fluid dynamics is crucial because of its ability to profoundly influence flow behavior and energy dissipation rate in various engineering contexts. The consequences of the power-law classification of *n*, *β* and *We* on the degree of skin friction versus *M* are shown in Figs 12 and 13, respectively. These graphs illustrate that as *M* as *n*, β, and increase, the skin friction improves proportionally with *M*. Figure 14 shows the varying values of *We* and β for the variation of skin friction versus *S*. As the values of β and *We* increase, the figure clearly shows that skin friction increases with *S*.

Nusselt numbers are dimensionless quantities that quantify convective heat transfer between solid surfaces and liquids. Brownian motion and thermophoresis, as shown in Fig.15, can significantly alter the Nusselt number. The rate of heat transfer decreases as *Nb* improves when plotted against *Nt* for different values of β and *We*. The efficiency of convective mass transfer can be determined by the Sherwood number. For several Brownian motion quantifiers, Fig.16 graphically shows the effect of mass transfer with *Nt*. Obviously, increasing the value of *Nb* speeds up the rate of mass transfer and decreases with *Nt*.

Table 1. Skin friction coefficient and Nusselt number versus Hartmann number, with $\beta = \infty$ and $Pr = 1$.

M	$-C_f Re_x^{\frac{1}{2}}$	$-\theta'(0)$
0	1.0005	0.5837
0.5	1.1182	0.5613
1.0	1.4142	0.5097
1.5	1.8028	0.4542
2.0	2.2361	0.4067
2.5	2.6926	0.3691
3.0	3.1623	0.3400
3.5	3.6401	0.3174
5	5.0990	0.2733
10	10.0499	0.2191
100	100.0050	0.1716
500	500.0010	0.1676

Table 2. Skin friction coefficient and Nusselt number versus n, β, We and M for the fixed values of $Nb = 0.001$, $Pr = 1$, $Nt = Le = S = 0$.

n	M	β	We	$-\frac{1}{2}C_f Re_x^{\frac{1}{2}}$	$-\theta'(0)$
0.0	0.0	∞	0.5	1.0005	0.5837
0.1	0.0	∞	0.5	0.9364	0.5711
0.2	0.0	∞	0.5	0.8584	0.5557
0.3	0.5	∞	0.2	0.8926	0.5178
0.3	1.0	∞	0.2	1.0773	0.4627
0.3	1.5	∞	0.2	1.2473	0.4071
0.3	0.5	10	0.3	1.2813	0.5314
0.3	1.0	5	0.3	1.4548	0.4911
0.3	1.5	1	0.3	2.2824	

Table 3. Nusselt number and Sherwood number versus Le, β, Nt, Nb, S and Pr for the fixed values of $We = n = M = 0$.

Pr	Nb	Nt	Le	β	S	$-\theta'(0)$	$-\phi'(0)$
1.6	0.1	0.1	1.0	∞	0.0	0.6953	0.3694
2.0						0.7732	0.4609
2.5						0.8492	0.5741
1.6	0.2					0.6395	0.6042
	0.3					0.5868	0.6814
	0.4	0.2				0.5110	0.6563
		0.3				0.4861	0.6023
		0.4	2.0			0.4098	1.0775
			2.5	0.1		0.4696	1.4780
				0.5		0.4420	1.4009
				1.0	0.1	0.4806	1.5833
					0.2	0.5354	1.8154
					0.3	0.5923	2.0571

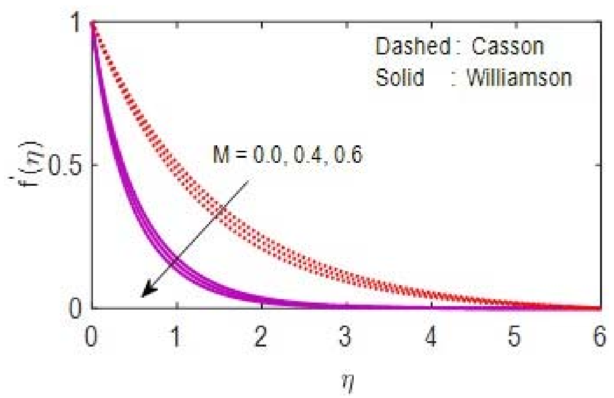

Fig.2. Impact of M on $f'(\eta)$.

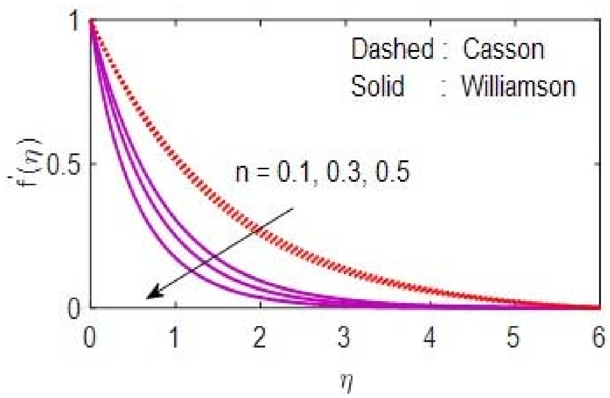

Fig.3. Impact of n on $f'(\eta)$.

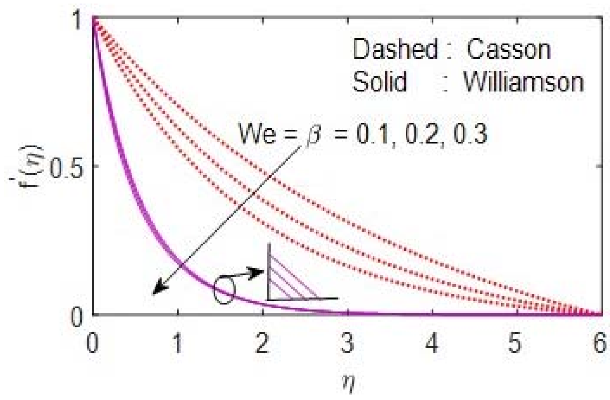

Fig.4. Impact of *We* and β on $f'(\eta)$.

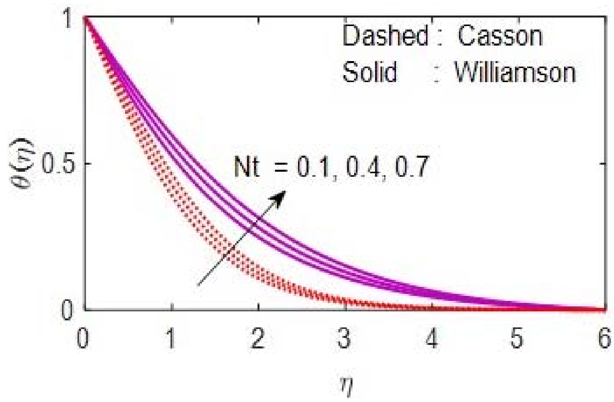

Fig.5. Impact of *Nt* on $\theta(\eta)$.

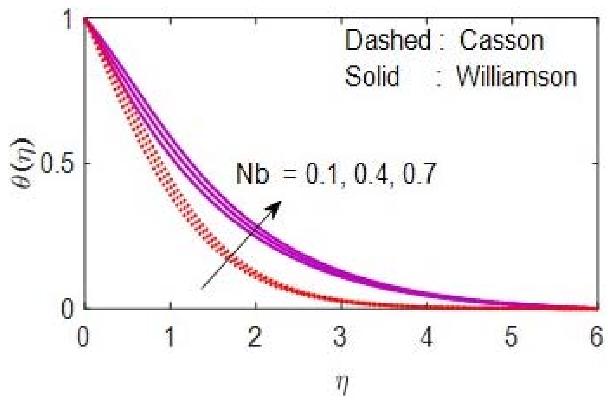

Fig.6. Impact of *Nb* on $\theta(\eta)$.

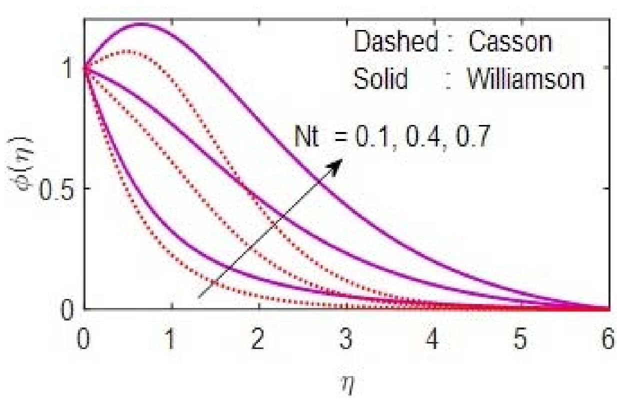

Fig.7. Impact of *Nb* on $\theta(\eta)$.

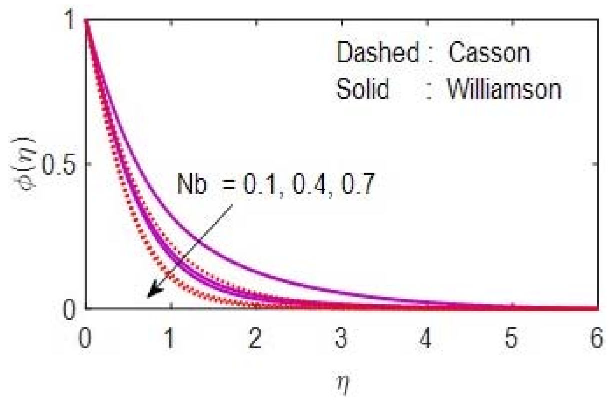

Fig.8. Impact of *Nb* on $\phi(\eta)$.

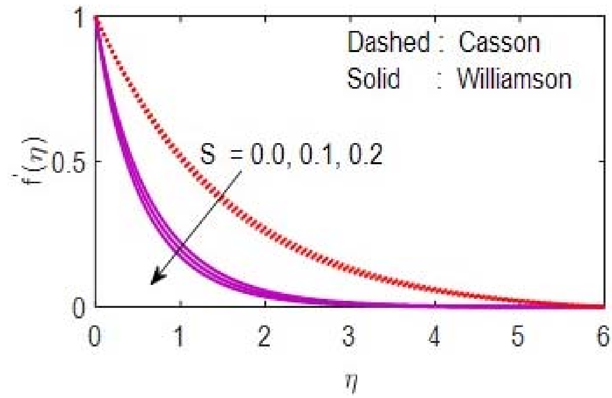

Fig.9. Impact of *S* on $f'(\eta)$.

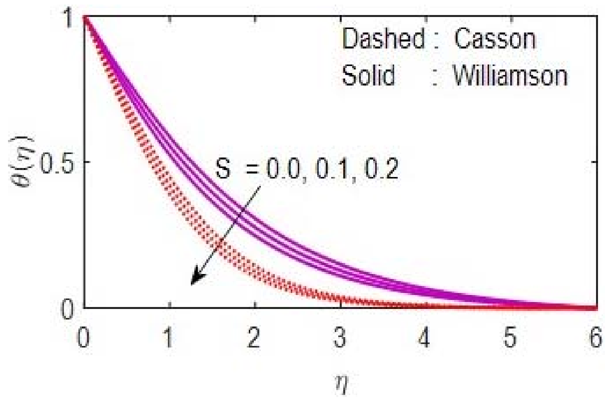

Fig.10. Impact of *S* on $\theta(\eta)$.

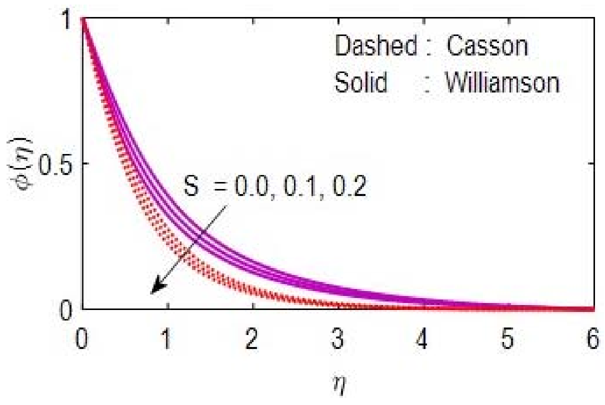

Fig.11. Impact of *S* on $\phi(\eta)$.

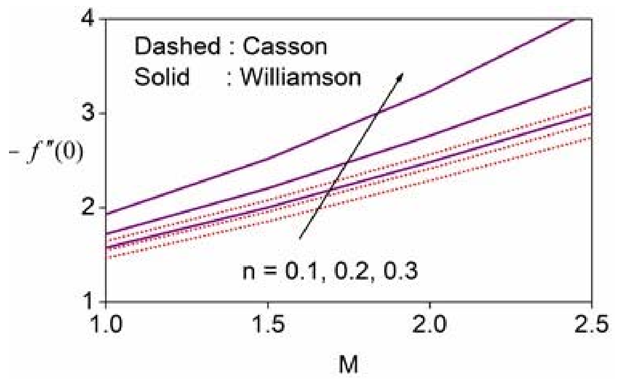

Fig.12. Impact of *M* and *n* on $-f''(0)$.

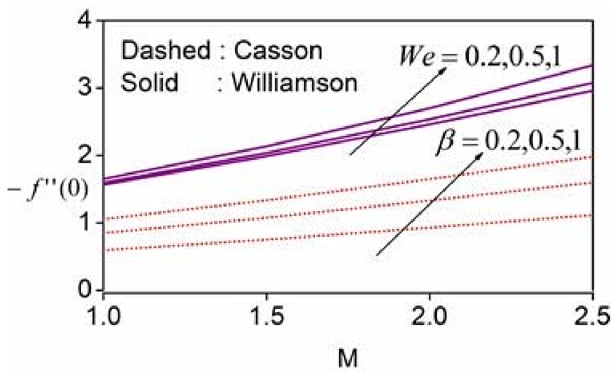

Fig.13. Impact of *M* and *We*, β on $-f''(0)$.

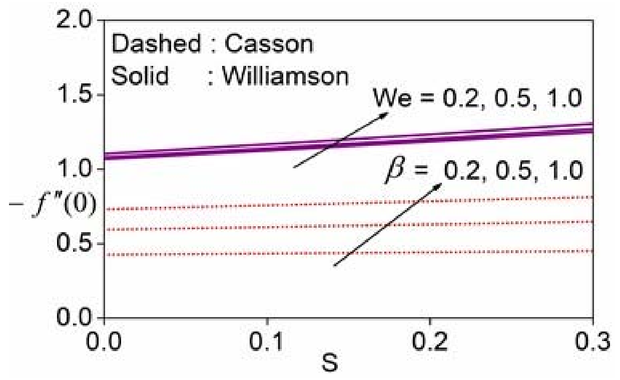

Fig.14. Impact of *S* and *We*, β on $-f''(0)$.

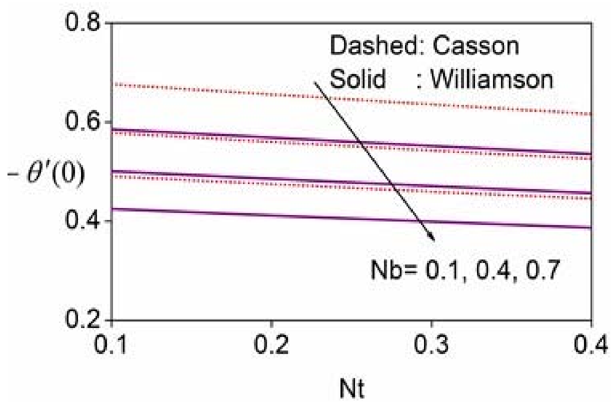

Fig.15. Impact of *Nt* and *Nb* on $-\theta'(0)$.

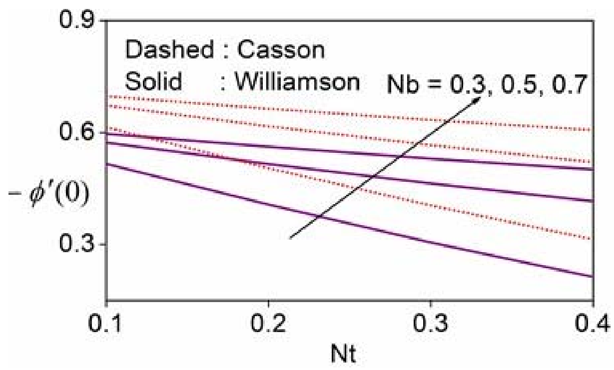

Fig.16. Impact of *Nt* and *Nb* on $-\phi'(0)$.

5. Conclusions

A non-Newtonian fluid whose constitutive equation holds true when shear rates are large and low for the tangential hyperbolic fluids. Thermophoresis and Brownian motion are included in the tangent hyperbolic model, and they both determine the nanofluid's dynamics. In the present work, numerical research on the magnetic field impact of the tangentially hyperbolic nanofluids through stretching sheets in a linear direction is reported. On this basis, a novel approach to the boundary value problem has been established. Here are the main results from the study:

1. *We* and β, together with the quantifiers *M* and *n*, reduce the velocity of the boundary layer thickness in both Casson and Williamson fluids.
2. The influence of *Nt* and *Nb* is to increase the temperature.
3. *Nt* has the effect of increasing the concentration, while *Nb* has the opposite effect.
4. An increase in the suction parameter leads to a decrease in the heat, concentration and velocity of the nanoparticles.
5. The property of *We* and β is to increase the skin friction coefficient.
6. In both the Casson and Williamson fluids, the frequency of mass transfer increases with the function *Nb*, but the rate of heat transfer decreases with the function *Nt*.

Limitations and Future scope

Complex industrial applications may not be fully captured by the model as it often assumes idealized geometry, such as flat stretched sheets. The reliability of many theoretical models cannot be established without considerable experimental validation.

Innovative applications and a better understanding of fluid behavior in many circumstances can be promoted through collaboration with materials science, nanotechnology and engineering experts in the field. Researchers can make progress in the field and discover new applications for MHD hyperbolic tangent Casson-Williamson nanofluid flows by addressing these limitations and exploring these future prospects.

Acknowledgements

The authors are deeply indebted to the editor and the anonymous reviewers, whose insightful remarks, helpful criticisms, and excellent ideas greatly improved the quality and clarity of the paper. Their critical reading and comments improved our technique, the way we presented our results and the overall quality of the paper. The time and effort they put into reviewing the paper is greatly appreciated. The authors also acknowledge the support of the management of SNIST, CVR and Anurag University in carrying out the present research work.

Nomenclature

C – concentration of nanoparticles

C_p – specific heat $(J / kg \cdot K)$

C_W – concentration at the surface

C_∞ – ambient concentration

D_B – Brownian motion coefficient

D_T – coefficient of thermophoresis diffusion

k – thermal conductivity of nanofluid

K^* – absorption coefficient

n – power law index

q_m – mass flux

q_w – heat flux

S – suction parameter

T – fluid temperature (K)

T_W – temperature at the surface

T_∞ – ambient temperature

(u, v) – velocity elements parallel to x and y axis

α – thermal diffusivity $\left(m^2 / sec\right)$

Γ – time constant

ν – kinetic viscosity $\left(m^2 / sec\right)$

ρ – density of the foundational liquid $\left(kg / m^3\right)$

σ^* – Stefan Boltzman constant

τ – ratio between nanomaterial heat capacity to fluid heat capacity

τ_w – shear stress

References

[1] Crane L.J. (1970): *Flow past a stretching plate*.– Z. für Angew. Math. Phys., ZAMP, vol.21, pp.645-647, https://doi.org/10.1007/BF01587695.

[2] Cortell R. (2005): *A note on magnetohydrodynamic flow of a power-law fluid over a stretching sheet*.– Appl. Math. Comput., vol.168, 557-566, https://doi.org/10.1016/j.amc.2004.09.046.

[3] Ahmed J., Shahzad A., Khan M. and Ali R. (2015): *A note on convective heat transfer of an MHD Jeffrey fluid over a stretching sheet*.– AIP Adv., vol.5, No.11, p.117117. https://doi.org/10.1063/1.4935571.

[4] Anwar I., Qasim A.R., Ismail Z., Salleh M.Z. and Shafie S. (2013). *Chemical reaction and uniform heat generation or absorption effects on MHD stagnation-point flow of a nanofluid over a porous sheet*.– World Applied Sciences Journal vol.24, No.10, pp.1390-1398, DOI:10.5829/idosi.wasj.2013.24.10.1307.

[5] Noorzadeh S., Moghanlou F.S., Vajdi M. and Ataei M. (2020). *Thermal conductivity, viscosity and heat transfer process in nanofluids: a critical review*.– J. Compos. Compd., vol.2, No.5, pp.175-192. https://doi.org/10.29252/jcc.2.4.3.

[6] Naikoti K. and Shashidar Reddy B. (2013): *MHD effects on non-Newtonian power-law fluid past a continuously moving porous flat plate with heat flux and viscous dissipation*.– International Journal of Applied Mechanics and Engineering, vol.18, No.2, pp.425-446.

[7] Saritha K., Rajasekhar M.N. and Shashidar Reddy B. (2015): *Quasi-linearization approach to effects of heat source/sink on MHD flow of non-Newtonian power-law fluid past a continuously moving porous flat plate with heat flux and viscous dissipation*.– International Journal of Applied Science and Engineering Research, vol.4, pp.36-56.

[8] Asogwa K.K. and Ibe A.A. (2020): *A study of MHD Casson fluid flow over a permeable stretching sheet with heat and mass transfer*.– J. Eng. Res. Rep., vol.16, No.2, pp.10-25, https://doi.org/10.9734/jerr/2020/v16i217161.

[9] Khan W.A. and Pop I. (2010): *Boundary-layer flow of a nanofluid past a stretching sheet*.– Int. J. Heat Mass Transf., vol.53, pp.2477-2483, https://doi.org/10.1016/j.ijheatmasstransfer.2010.01.032.

[10] Kuznetsov A.V. and Nield D.A. (2010): *Natural convective boundary-layer flow of a nanofluid past a vertical plate*. Int. J. Therm. Sci., vol.49, pp.243-247, https://doi.org/10.1016/j.ijthermalsci.2009.07.015.

[11] Mabood F., Khan W.A. and Ismail A.I.M. (2015): *MHD boundary layer flow and heat transfer of nanofluids over a nonlinear stretching sheet: a numerical study*.– J. Magn. Magn. Mater., vol.374, pp.569-576, https://doi.org/10.1016/j.jmmm.2014.09.013.

[12] Akolade M., Adeosun T. and Olabode J. (2020): *Influence of thermophysical features on MHD squeezed flow of dissipative Casson fluid with chemical and radiative effects*.– J. Appl. Comput. Mech., vol.7, No.4, pp.1999-2009, https://doi.org/10.22055/jacm.2020.34909.2508.

[13] Sheikholeslami M., Hayat T. and Alsaedi A. (2016): *MHD free convection of Al2O3-water nanofluid considering thermal radiation: A numerical study*.– Int. J. Heat Mass Transf., vol.96, pp.513-524. https://doi.org/10.1016/j.ijheatmasstransfer.2016.01.059.

[14] Siti Khuzaimah S., Seripah Awang K., Ahmad Haziq Mad S., Nur Zulaikha I. and Siti Nur Saiyidah Ab.H. (2012): *Hydromagnetic boundary layer flow over stretching surface with thermal radiation*.– World Applied Sciences Journal vol.17, pp.33-38.

[15] Hayat T., Bashir G., Waqas M. and Alsaedi A. (2016): *MHD 2D flow of Williamson nanofluid over a nonlinear variable thicked surface with melting heat transfer*.– Journal of Molecular Liquids, vol.223, pp.836-844, https://doi.org/10.1016/j.molliq.2016.08.104.

[16] Khan M., Malik M.Y., Salahuddin T., Rehman K.U., Naseer M. and Khan I. (2017): *MHD flow of Williamson nanofluid over a cone and plate with chemically reactive species*.– J. Mol. Liq. vol.231, pp.580-588, https://doi.org/10.1016/j.molliq.2017.02.031.

[17] Malik M.Y., Salahuddin T., Hussain A. and Bilal S. (2015): *MHD flow of tangent hyperbolic fluid over a stretching cylinder: using Keller Box method*.– J. Magn. Magn. Mater., vol.395, pp.271-276, https://doi.org/10.1016/j.jmmm.2015.07.097.

[18] Akbar N.S., Nadeem S., Haq R.U. and Khan Z.H. (2013): *Numerical solutions of magnetohydrodynamic boundary layer flow of tangent hyperbolic fluid towards a stretching sheet*.– Indian J. Phys., vol.87, pp.1121-1124, https://doi.org/10.1007/s12648-013-0339-8.

[19] Idowu A.S., Akolade M.T., Abubakar J.U. and Falodun B.O. (2020): *MHD free convective heat and mass transfer flow of dissipative Casson fluid with variable viscosity and thermal conductivity effects*.– J. Taibah Univ. Sci., vol.14, pp.851-862, https://doi.org/10.1080/16583655.2020.1781431.

[20] Gbadeyan J.A., Titiloye E.O. and Adeosun A.T. (2020). *Effect of variable thermal conductivity and viscosity on Casson nanofluid flow with convective heating and velocity slip*.– Heliyon, vol.6, e03076, https://doi.org/10.1016/j.heliyon.2019.e03076.

[21] Asogwa K.K., Goud B.S., Redd Y.D. and Ibe A.A. (2022): *Suction effect on the dynamics of EMHD Casson nanofluid over an induced stagnation point flow of stretchable electromagnetic plate with radiation and chemical reaction*.– Results Eng., vol.15, p.100518. https://doi.org/10.1016/j.rineng.2022.100518.

[22] Ghadikolaei S.S., Hosseinzadeh Kh., Ganji D.D. and Jafari B. (2018): *Nonlinear thermal radiation effect on magneto Casson nanofluid flow with Joule heating effect over an inclined porous stretching sheet*.– Case Stud. Therm. Eng., vol.12, pp.176-187, https://doi.org/10.1016/j.csite.2018.04.009.

[23] Haq R., Nadeem S., Khan Z. and Okedayo T. (2014): *Convective heat transfer and MHD effects on Casson nanofluid flow over a shrinking sheet*.– Open Phys., vol.12, https://doi.org/10.2478/s11534-014-0522-3.

[24] Shashidar Reddy B., Saritha K., and Venkata Madhu J. (2020): *Impact of chemical reaction on mass transfer and melting heat transfer of porous MHD Casson fluid flow*.– Journal of Mathematical and Computational Science, vol.11, No.1, pp.149-164.

[25] Mabood F., Khan W.A. and Ismail A.I.Md. (2015): *MHD stagnation point flow and heat transfer impinging on stretching sheet with chemical reaction and transpiration*.– Chem. Eng. J., vol.273, pp.430-437, https://doi.org/10.1016/j.cej.2015.03.037.

[26] Hayat T., Bilal Ashraf M., Shehzad S. and Alsaedi A. (2015): *Mixed convection flow of Casson nanofluid over a stretching sheet with convectively heated chemical reaction and heat source/sink*.– J. Appl. Fluid Mech., vol.8, pp.803-813, https://doi.org/10.18869/acadpub.jafm.67.223.22995.

[27] Khan M., Hussain A., Malik M.Y. Salahuddin T. and Khan F. (2017): *Boundary layer flow of MHD tangent hyperbolic nanofluid over a stretching sheet: a numerical investigation*.– Results Phys., vol.7, pp.2837-2844, https://doi.org/10.1016/j.rinp.2017.07.061.

[28] Reddy C.S., Naikoti K. and Rashidi M.M. (2017): *MHD flow and heat transfer characteristics of Williamson nanofluid over a stretching sheet with variable thickness and variable thermal conductivity*.– Trans. Razmadze Math. Inst., vol.171, pp.195-211, https://doi.org/10.1016/j.trmi.2017.02.004.

[29] Nadeem S. and Hussain S.T. (2014): *Heat transfer analysis of Williamson fluid over exponentially stretching surface*.– Appl. Math. Mech., vol.35,pp.489-502, https://doi.org/10.1007/s10483-014-1807-6.

[30] Li Y.-X., Alshbool M.H., Lv Y.-P., Khan I., Riaz Khan M. and Issakhov A. (2021): *Heat and mass transfer in MHD Williamson nanofluid flow over an exponentially porous stretching surface*.– Case Stud. Therm. Eng., vol.26, p.100975, https://doi.org/10.1016/j.csite.2021.100975.

[31] Muzara H. and Shateyi S. (2023): *Magnetohydrodynamics Williamson nanofluid flow over an exponentially stretching surface with a chemical reaction and thermal radiation*.– Mathematics, vol.11, p.2740, https://doi.org/10.3390/math11122740.

[32] Zhu A., Ali H., Ishaq M., Junaid M.S., Raza J. and Amjad M. (2022): *Numerical study of heat and mass transfer for williamson nanofluid over stretching/shrinking sheet along with brownian and thermophoresis effects*.– Energies, vol.15, p.5926, https://doi.org/10.3390/en15165926.

[33] Humane P.P., Patil V.S. and Patil A.B. (2021): *Chemical reaction and thermal radiation effects on magnetohydrodynamics flow of Casson-Williamson nanofluid over a porous stretching surface*.– Proc. Inst. Mech. Eng., Part E, J. Process Mech. Eng., vol.235, pp.2008-2018, https://doi.org/10.1177/09544089211025376.

[34] Rajeswari P.M. and De P. (2024): *Shape factor and sensitivity analysis on stagnation point of bioconvective tetra-hybrid nanofluid over porous stretched vertical cylinder*.– BioNanoSci., vol.14, pp.3035-3058, https://doi.org/10.1007/s12668-024-01586-8.

[35] Pattnaik P.K., Mishra S.R., Baithalu R. and Panda S. (2024): *Sensitivity analysis and enhanced EMHD performance of unsteady ferrite-water hybrid nanofluid on a Riga plate with variable magnetization and heat generation*.– Numerical Heat Transfer, Part A: Applications, pp.1-23, https://doi.org/10.1080/10407782.2024.2363503.

[36] Mishra S.R., Pattnaik P.K., Bhatti M.M. and Abbas T. (2017): *Analysis of heat and mass transfer with MHD and chemical reaction effects on viscoelastic fluid over a stretching sheet*.– Indian J. Phys., vol.91, pp.1219-1227, https://doi.org/10.1007/s12648-017-1022-2.

[37] Bartwal P., Upreti H. and Pandey A.K. (2024): *Insight into the impact of melting heat transfer and MHD on stagnation point flow of tangent hyperbolic fluid over a porous rotating disk*.– Journal of Porous Medium, vol.27, No.9, pp.73-100, DOI: 10.1615/JPorMedia.2024051926.

[38] Bartwal P., Upreti H. and Pandey A.K. (2024): *Exploring the features of Von-Karman flow of tangent hyperbolic fluid over a radially stretching disk subject to heating due to porous media and viscous heating*.– Modern Physics Letters B, vol.38, No.18, p.2450135, https://doi.org/10.1142/S0217984924501355.

[39] Puchakayala S.R., Borra S.R., Kallu S., Formanova S., Iyaz Khan M., Waqas M., Ahmad F., and Gupta M. (2024): *Comparative numerical study featuring magnetized nanofluids configured by elongating sheet with thermophoresis and Brownian motion*.– Partial Differential Equations in Applied Mathematics, p.100915, https://doi.org/10.1016/j.padiff.2024.100915.

[40] Pattnaik P.C., Mishra S.R. and Pattanik P.K. (2022): *Impact of radiative and dissipative heat on the Williamson nanofluid flow within a parallel channel due to thermal buoyancy*.– Proceedings of the Institution of Mechanical Engineers, Part N: Journal of Nanomaterials, Nanoengineering and Nanosystems, vol.236, No.1-2, pp.3-18, https://doi.org/10.1177/23977914221080046.

[41] Shanker Goud B., Dharmendar Reddy Y. and Mishra S.R. (2023): *Joule heating and thermal radiation impact on MHD boundary layer Nanofluid flow along an exponentially stretching surface with thermal stratified medium*.– Proceedings of the Institution of Mechanical Engineers, Part N: Journal of Nanomaterials, Nanoengineering and Nanosystems, vol.237, No.3-4, pp.107-119, https://doi.org/10.1177/23977914221100.

[42] Thirupathi T., Mishra S.R., Ali Abbas M., Bhatti M.M. and Abdelsalam A.I. (2022): *Three-dimensional nanofluid stirring with non-uniform heat source/sink through an elongated sheet*.– Applied Mathematics and Computation, vol.421, p.126927, https://doi.org/10.1016/j.amc.2022.126927.

[43] Mishra A.K., Pattnaik P.K., Mishra S.R. and Senapati N. (2021): *Dissipative heat energy on Cu and Al2O3 ethylene-glycol-based nanofluid flow over a heated semi-infinite vertical plate*.– Journal of Thermal Analysis and Calorimetry, vol.145, No.1, pp.129-137, https://doi.org/10.1007/s10973-020-09666-z.

[44] Yousef N.S., Megahed A.M., Ghoneim N.I., Elsafi M. and Fares E. (2022): *Chemical reaction impact on MHD dissipative Casson-Williamson nanofluid flow over a slippery stretching sheet through porous medium*.– Alex. Eng. J., vol.61, pp.10161-10170, https://doi.org/10.1016/j.aej.2022.03.032.

[45] Baag S., Panda S., Pattnai, P.K. and Mishra S.R. (2023): *Free convection of conducting nanofluid past an expanding surface with heat source with convective heating boundary conditions*. International Journal of Ambient Energy, vol.44, No.1, pp.880-891, https://doi.org/10.1080/01430750.2022.2156607.

[46] Pattnaik P.K., Mishra S.R., Panda S., Syed S.A. and Muduli K. (2022): *Hybrid methodology for the computational behaviour of thermal radiation and chemical reaction on viscoelastic nanofluid flow*.– Mathematical Problems in Engineering, Article ID 2227811, https://doi.org/10.1155/2022/2227811.

[47] Panda S., Surender O., Mishra S.R. and Pattnaik P.K. (2023): *Response surface methodology and sensitive analysis for optimizing heat transfer rate on the 3D hybrid nanofluid flow through permeable stretching surface*.– Journal of Thermal Analysis and Calorimetry, vol.148, No.14, pp.7369-7382, https://doi.org/10.1007/s10973-023-12183-4.

[48] Seema T., Mishra S.R. and Sharma R.P. (2022): *Simulation of time-dependent radiative heat motion over a stretching/shrinking sheet of hybrid nanofluid: stability analysis for dual solutions*.– Proceedings of the Institution of Mechanical Engineers, Part N: Journal of Nanomaterials, Nanoengineering and Nanosystems, vol.236, No.1-2, pp.19-30, https://doi.org/10.1177/23977914211069021.

[49] Anwar M.I., Shafie S., Hayat T., Shehzad S.A. and Salleh M.Z. (2017*): Numerical study for MHD stagnation-point flow of a micropolarnanofluid towards a stretching sheet*.– J. Braz. Soc. Mech. Sci. Eng., vol.39, pp.89-100, https://doi.org/10.1007/s40430-016-0610-y.

[50] Gomathi N. and De P. (2024): *Entropy optimization on EMHD Casson Williamson penta-hybrid nanofluid over porous exponentially vertical cone*.– Alexandria Engineering Journal, vol.108, pp.590-610, https://doi.org/10.1016/j.aej.2024.07.092.

[51] Singh K., Pandey A.K. and Kumar M. (2021): *Numerical solution of micropolar fluid flow via stretchable surface with chemical reaction and melting heat transfer using Keller-Box method*.– Propulsion and Power Research, vol.10, No.2, pp.194-207, https://doi.org/10.1016/j.jppr.2020.11.006.

Received: August 5, 2024
Revised: February 7, 2025